Control of protein trafficking by reversible masking of transport signals

Omer Abraham[a,†], Karnit Gotliv[a,†], Anna Parnis[a], Gaelle Boncompain[b], Franck Perez[b], and Dan Cassel[a,*]

[a]Department of Biology, Technion, Haifa 320003, Israel; [b]Institut Curie, Centre de Recherche, PSL Research University, and CNRS, UMR144, Paris 75248, France

ABSTRACT **Systems that allow the control of protein traffic between subcellular compartments have been valuable in elucidating trafficking mechanisms. Most current approaches rely on ligand or light-controlled dimerization, which results in either retardation or enhancement of the transport of a reporter. We developed an alternative approach for trafficking regulation that we term "controlled unmasking of targeting elements" (CUTE). Regulated trafficking is achieved by reversible masking of the signal that directs the reporter to its target organelle, relying on the streptavidin–biotin system. The targeting signal is generated within or immediately after a 38–amino acid streptavidin-binding peptide (SBP) that is appended to the reporter. The binding of coexpressed streptavidin to SBP causes signal masking, whereas addition of biotin causes complex dissociation and triggers protein transport to the target organelle. We demonstrate the application of this approach to the control of nuclear and peroxisomal protein import and the generation of biotin-dependent trafficking through the endocytic and COPI systems. By simultaneous masking of COPI and endocytic signals, we were able to generate a synthetic pathway for efficient transport of a reporter from the plasma membrane to the endoplasmic reticulum.**

Monitoring Editor
Benjamin S. Glick
University of Chicago

Received: Jul 13, 2015
Revised: Feb 4, 2016
Accepted: Feb 23, 2016

INTRODUCTION

Eukaryotic cells contain multiple subcellular compartments, each with its typical lipid and protein composition. Proteins may reside in a compartment persistently or shuttle between two or more locations. Targeting of proteins to their destination is frequently dictated by short, linear peptide motifs (Pandey, 2010). These motifs are recognized by receptors/adaptors that mediate insertion into the target organelle or, in the case of the secretory system, incorporation into the correct transport vesicle.

The synthesis and transport of proteins are typically continuous processes, whereas controlled delivery of proteins to their destination can be beneficial for both basic research and biotechnological applications. To this end, researchers have developed various techniques for transport control and synchronization. In the secretory system, a block at low temperatures has been used to synchronize anterograde traffic from the ER–Golgi intermediate compartment (ERGIC; Saraste and Kuismanen, 1984; Lotti *et al.*, 1992; Klumperman *et al.*, 1998) or the *trans*-Golgi network (TGN; Matlin and Simons, 1983; Saraste *et al.*, 1986; Griffiths *et al.*, 1989), and the use of the temperature-sensitive (ts) mutant of the viral glycoprotein vesicular stomatitis virus G (VSV-G) has allowed follow-up of synchronized exit from the endoplasmic reticulum (ER; Bergmann *et al.*, 1981; Bergmann, 1989; Lodish and Kong, 1983; Presley *et al.*, 1997). Recently more versatile approaches were introduced that are generally based on manipulation of protein localization by the introduction of controllable dimerization elements (Rakhit *et al.*, 2014). Dimerization is controlled by a small ligand or by light, allowing for trigger-dependent transport by mechanisms such as reversible retention of the transported protein due to self-aggregation (Rivera *et al.*, 2000; Al-Bassam *et al.*, 2012; Chen *et al.*, 2013) and piggyback transport by dimerization with a carrier protein bearing a transport signal (Geda *et al.*, 2008; Beyer *et al.*, 2015). In a study aimed at regulating transport in the secretory pathway

This article was published online ahead of print in MBoC in Press (http://www.molbiolcell.org/cgi/doi/10.1091/mbc.E15-07-0472) on March 3, 2016.

†These authors contributed equally to this work.

*Address correspondence to: Dan Cassel (danc@tx.technion.ac.il).

Abbreviations used: CUTE, controlled unmasking of targeting elements; SA, streptavidin; SBP, streptavidin-binding peptide.

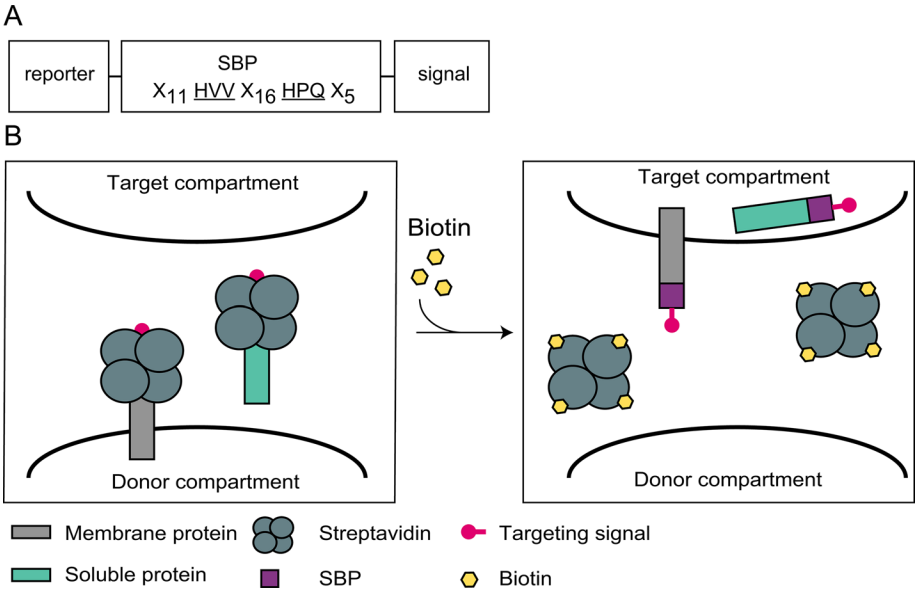

FIGURE 1: Design of a system for reversible masking of transport signals. (A) Scheme of the SBP-based constructs. The two amino acid triplets of SBP that interact with the biotin-binding sites of SA (Barrette-Ng *et al.*, 2013) are underlined. (B) Schematic representation of the CUTE approach. When targeting signals are appended to SBP, binding of SA may hinder the signals and thus prevent transport to the target compartment. Biotin-induced SA dissociation from SBP would then lead to unmasking of the signal, followed by synchronous transport.

(Boncompain *et al.*, 2012), tagging of one protein with streptavidin (SA) and the other with the streptavidin-binding peptide (SBP) was used to trap a reporter protein in the ER or the Golgi apparatus through interaction with an organelle-resident membrane protein that served as a "hook." Synchronized transport could be triggered by the addition of biotin, which causes dissociation of the SA-SBP complex. Although this system is highly effective for following anterograde transport in the secretory system, it is less suitable for following transport in the reverse direction (e.g., COPI-mediated Golgi-to-ER transport), as the hook–reporter complex will be subjected to continuous retrograde transport, thus impairing the functioning of the hook.

Here we describe a novel application of the SA-SBP system for controlled intracellular transport based on reversible masking of transport signals. We demonstrate the applicability of this approach to diverse transport events, including nuclear and peroxisomal import, as well as to retrograde Golgi-to-ER and endocytic transport.

RESULTS

The SBP binds SA with high affinity (Wilson *et al.*, 2001). This 38–amino acid (aa) peptide has two critical SA-binding sites separated by a 16-aa stretch that mostly acts as a spacer but also displays several interactions with SA (Figure 1A; Barrette-Ng *et al.*, 2013). We envisaged that binding of the tetrameric SA to SBP might impose steric hindrance on short signals appended in proximity to one of the major SA-binding sites. To test this idea, we appended SBP followed by a trafficking signal to the carboxy termini of both membrane and soluble reporter proteins (Figure 1B). Masking of the signals upon SA binding is expected to abrogate the targeting function of the signals, whereas subsequent addition of biotin should cause dissociation of the SA-SBP complex, signal exposure, and initiation of reporter transport.

Regulated uptake of proteins from cytosol to organelles

We initially sought to test the controlled unmasking of targeting elements (CUTE) approach using a rapid and readily tractable system and chose nuclear import using the SV-40 large T antigen nuclear localization signal (NLS). A green fluorescent protein x3 (GFPx3) reporter (Sakakida *et al.*, 2005) was fused to SBP followed by the KKKRKV NLS. This fusion protein was coexpressed with the core domain of SA in HeLa cells at a 1:10 plasmid ratio. Because expression of soluble SA in mammalian cells has not been previously documented, we analyzed the expressed protein and observed that it was in the correct tetrameric form (Supplemental Figure S1A) and was diffusely distributed in the cytoplasm (Supplemental Figure S1B).

The GFPx3-SBP-NLS fusion showed the expected nuclear localization, whereas cotransfection with SA resulted in a largely cytosolic pattern of GFP fluorescence (Figure 2A). On addition of biotin, the protein became concentrated in the nucleus in a manner that resembled that observed in cells that did not coexpress SA. Measurements of the nuclear-to-cytosolic fluorescence ratio in multiple cells (Figure 2B) showed a clear shift to lower ratios in cells expressing SA, which was reversed upon addition of biotin. Kinetic analysis (Figure 2, C and D, and Supplemental Movie S1) showed that uptake into the nucleus is preceded by a lag period of ~5 min and reaches half-maximal values within ~15 min. Thus reversible masking of an NLS was attained using the SBP-SA–based approach. Binding of SA in itself does not prevent nuclear entry, as efficient import was observed in constructs in which masking was abrogated due to the introduction of a linker between SBP and NLS (see later discussion of Figure 10).

Another short signal that acts autonomously in import into an organelle is the carboxy-terminal SKL sequence, which is known to direct peroxisomal import from cytosol through the PTS1 system (Wilson *et al.*, 2001; Smith and Aitchison, 2013). As shown in Figure 3A, a GFP-SBP-SKL fusion protein displayed the expected peroxisome-like distribution, which depended on the SKL signal and overlapped that of the peroxisomal marker red fluorescent protein (RFP)–SKL. However, when coexpressed with SA, the fusion protein displayed diffuse cytosolic distribution; upon biotin addition, the construct redistributed into a peroxisomal pattern (Figure 3B). Microscopic observation revealed that 96 ± 2% of the transfected cells showed a nonpunctate, diffuse pattern in the presence of SA, whereas essentially all cells showed a peroxisomal pattern after biotin treatment. Peroxisomal uptake was rather slow, reaching maximal levels after 3–4 h (Figure 3C and Supplemental Movie S2). A similar kinetics of peroxisomal import was previously observed using microinjected reporters (Walton *et al.*, 1992).

Masking/unmasking of COPI dilysine signals

We next sought to test whether the masking/unmasking approach could be applied to the secretory system. We initially tested the applicability of this approach to the COPI system, which mediates retrograde transport from the ERGIC elements and the Golgi apparatus. To this end, we used as reporter the type I plasma membrane

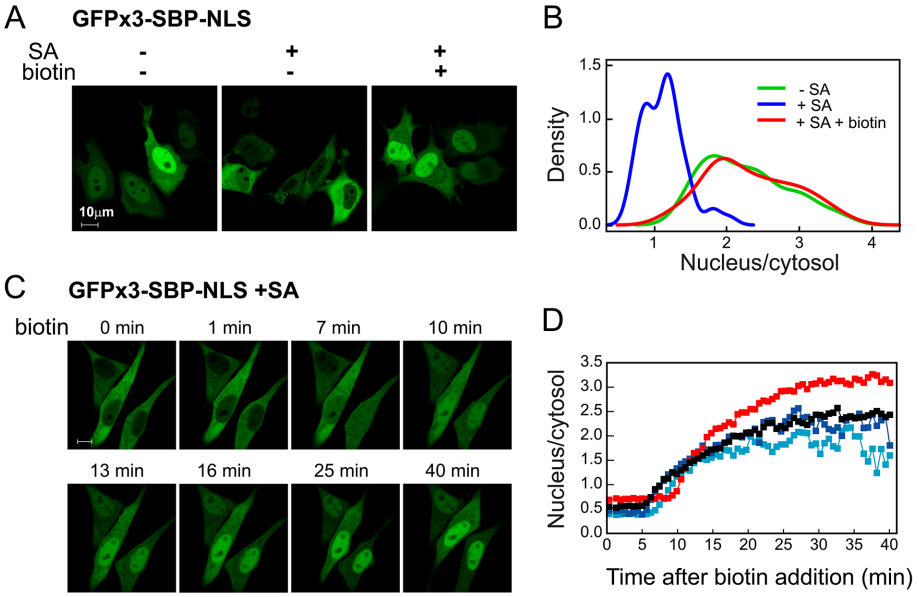

FIGURE 2: Masking/unmasking of a signal for nuclear import. (A) Biotin-induced nuclear import. HeLa cells were transfected with 3xGFP-SBP-NLS with or without SA (plasmid ratio, 1:10). At 24 h later, biotin (400 μM) was added where indicated, and incubation proceeded for 1 h. (B) Quantification of biotin-induced nuclear import. Conditions as in A. Nuclear-to-cytosolic ratios were measured on 50 individual cells for each condition as described in *Materials and Methods*. Density plots (smoothed histograms) were generated using kernel smoothing under the R console. (C) Live-cell imaging of biotin-induced nuclear import. Conditions as in A. Images were taken from Supplemental Movie S1. (D) Time course of biotin-induced nuclear import as observed in four cells.

protein CD4, with GFP and SBP fused at its cytoplasmic tail. Following the SBP sequence we appended a dilysine signal of the K(X)KXX-COOH type, which is known to mediate COPI-dependent retrograde transport of membrane proteins through direct binding to the COPI coat (Letourneur *et al.*, 1994; Jackson *et al.*, 2012; Ma and Goldberg, 2013). When exposed, the dilysine signal is expected to result in a largely ER distribution of the reporter, whereas signal masking should result in transport to the plasma membrane. Two signals were used: KKTN, a widely used signal derived from the *Saccharomyces cerevisiae* ER-resident WBP1 protein, and a KRKAE sequence that is present in several reticulon proteins and was found in our lab to function as a potent ER retrieval signal. In transiently transfected HeLa cells, SBP-KKTN/KRKAE–tagged CD4-GFP showed the expected ER localization, with no detectable surface-exposed antigen (Figure 4A). However, when cotransfected with SA, the CD4 construct was efficiently transported to the plasma membrane (PM), indicating that SA binding to SBP masked the dilysine signal. When biotin was added soon after transfection, PM expression was prevented, and the reporter showed ER localization. A similar experiment was performed using the ts VSVG mutant (VSVGts045), which is retained in the ER at 40°C and is synchronously released upon shift to the permissive temperature. When VSVGts045-GFP-SBP-KRKAE was incubated overnight at 40°C and then shifted for 3 h to a permissive temperature of 32°C, it retained its ER localization pattern, whereas its coexpression with streptavidin led to transport to the plasma membrane (Figure 4B, two middle images). For reasons that are as yet unclear, a minor portion of VSVGts045-GFP-SBP-KRKAE remained ER localized in the presence of streptavidin, despite the addition of cycloheximide upon temperature shift to prevent new protein synthesis. Significantly, the addition of biotin upon shift to the permissive temperature completely prevented the transport of VSVGts045 to the plasma membrane in virtually all cells examined, demonstrating that biotin can reverse the SA-induced masking (Figure 4B, right).

Thus far, we demonstrated that dilysine signals appended to SBP become masked upon SA binding and that masking can be reversed by biotin. To follow the retrograde transport step, one should initially apply conditions that allow the reporter to accumulate at a post-ER compartment. Seeking to follow retrograde transport from the Golgi, we first accumulated cells coexpressing SA and a VSVGts045 construct with appended SBP-KRKAE in the ER by overnight incubation at 40°C and then switched them to the permissive temperature (32°C) for a limited period of 1 h, a period that was found optimal for Golgi accumulation. To specifically follow transport originating from the Golgi, we used a construct based on the photoconvertible fluorescent protein Dendra2 in place of GFP (VSVGts045-Dendra2-SBP-KRKAE). After reaching the Golgi, the Dendra2 protein was irradiated at the Golgi area, resulting in the conversion of fluorescence from green to red (Figure 5). After additional incubation at 32°C, the red fluorescence gradually disappeared from the Golgi and appeared at the plasma membrane (Figure 5B, top); the green fluorescence followed a similar course with some delay, apparently representing new synthesis of the reporter. Unmasking the dilysine

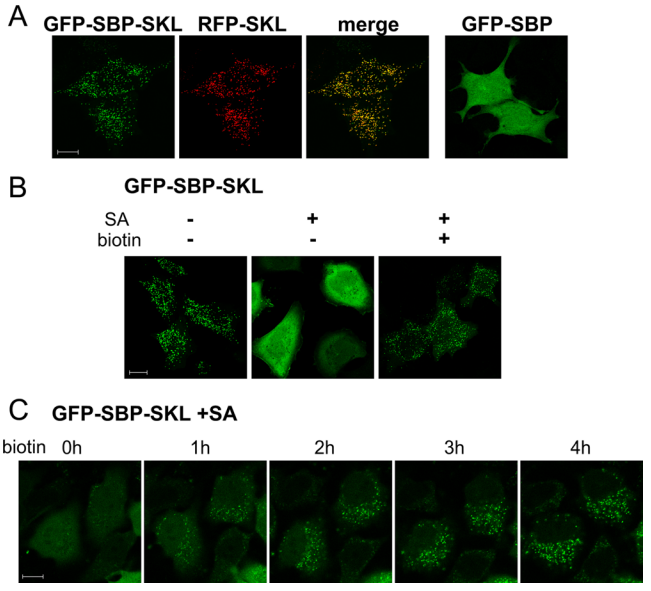

FIGURE 3: Masking/unmasking of a signal for peroxisomal import. (A) GFP-SBP-SKL localizes to peroxisomes. GFP-SBP-SKL was cotransfected with the peroxisomal marker RFP-SKL. GFP-SBP (without SKL) served as a control. (B) Biotin-dependent import into peroxisomes. GFP-SBP-SKL was cotransfected with SA (plasmid ratio, 1:10) and cells were incubated for 4 h with or without biotin in the presence of cycloheximide. (C) Live imaging of biotin-induced peroxisomal import. Images were taken from Supplemental Movie S2.

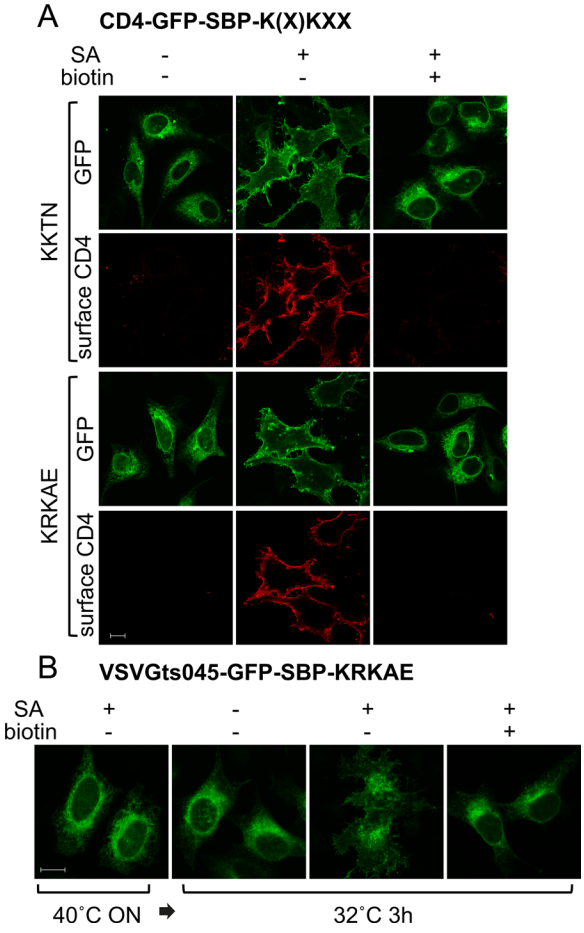

FIGURE 4: Masking/unmasking of a Golgi-to-ER retrieval signal. (A) HeLa cells were transfected with CD4-GFP-SBP-KKTN (top) or CD4-GFP-SBP-KRKAE (bottom) with or without SA (plasmid ratio, 3:2) and biotin. After overnight incubation, cells were incubated for an additional 3 h in the presence of cycloheximide, fixed (but not permeabilized), and stained with anti-CD4 antibody. (B) Cells were transfected with VSVGts045-GFP-SBP-KRKAE with or without streptavidin (plasmid ratio, 3:2). After overnight incubation at 40°C, the cells were switched to the permissive temperature of 32°C for 3 h in the presence of cycloheximide with or without biotin.

signal with biotin just before photoconversion led to redistribution to the ER without any plasma membrane accumulation (Figure 5, bottom). Some biotin-induced redistribution from the Golgi to the ER could be observed after 1 h, reaching its maximal extent after 3–4 h; however, due to the relatively weak signal, the precise kinetics of the transport was difficult to determine. We conclude that the masking/unmasking approach allows for follow-up of ligand-dependent retrograde trafficking of membrane proteins from the Golgi to the ER.

Endocytic signals

Clathrin-dependent endocytosis of membrane proteins depends on the presence of short signals of various types at their cytoplasmic tail (Bonifacino and Traub, 2003). We looked for an endocytic signal that could be integrated within the SBP sequence and thus be subject to direct masking on SA binding. As mentioned, the two major SA-binding sites in SBP are flanked by a stretch that adopts a helical conformation when bound to SA. This stretch is believed to function primarily as a spacer between biotin-binding sites on two SA subunits, although some of the residues in this stretch contribute to SBP-SA interaction (Barrette-Ng *et al.*, 2013). Inspecting the SBP sequence, we decided to attempt to create an acidic-dileucine endocytic signal of the [DE]XXXLL consensus by mutating the **Q**LRAR**L** sequence within the connecting helix to **E**LRA**L**L (Figure 6A). Analysis of the published SBP-SA structure (accession number 4JO6) using the Chimera package (Pettersen *et al.*, 2004) indicated that the Q-to-E mutation should not affect the SBP-SA interaction, whereas the R-to-L mutation is expected to result in loss of one hydrogen bond. We first tested whether the modified SBP (SBP_{EL}) provides an endocytic signal by fusing it to CD4 whose cytoplasmic tail was truncated to remove the endogenous endocytic signal ($CD4_{1–429}$; Figure 6). Cells were incubated for 1 h in the cold with Alexa 488–labeled anti-CD4 antibodies to allow for antibody binding and then switched back to 37°C for 20 min to allow for antibody uptake. Texas Red–conjugated transferrin was used as endocytic marker. As shown in Figure 6B, in cells expressing the truncated CD4 construct with nonmutated SBP, the antibody remained at the cell surface. By contrast, cells expressing $CD4_{1–429}$-SBP_{EL} or wild-type CD4 showed antibody uptake to endocytic structures, most of which contained labeled transferrin.

We next tested whether the endocytic signal we embedded within SBP can be subjected to reversible masking. We transfected cells with $CD4_{1–429}$-SBP_{EL} with or without SA and followed uptake of Alexa 488–labeled anti-CD4 antibody in the presence or absence of biotin. At the end of the incubation, antibody that remained at the cell surface was detected with cy3-conjugated secondary antibody (Figure 7A). Efficient internalization and disappearance of antibody from the cell surface was observed in cells that had not been transfected with SA, whereas cotransfection with SA largely prevented antibody uptake. The apparent ability of SA to prevent internalization indicates that the mutated SBP_{EL} can still efficiently interact with SA. Addition of biotin reversed the effect of SA, resulting in synchronized internalization. Measurement of the intensities in the red and green channels (reflecting external and total antigen, respectively; Figure 7B) indicated a masking efficiency for SA of ~75%; unmasking with biotin caused a decrease in the external-to-internal fluorescence ratio to a low level that resembled that in control cells not transfected with SA. Live-cell imaging revealed that $CD4_{1–429}$-SBP_{EL}–bound antibody was rapidly internalized upon biotin-induced release from masking by SA (Figure 7C). After 10 min, part of the antibody fluorescence started to appear in a juxtanuclear position (Figure 7C and Supplemental Movie S3), which largely coincided with that of the Golgi/TGN markers GalT and TGN46 at 30 min (Figure 7D). It thus appears that the endocytic signal that we created may also direct endosome-to-TGN retrograde transport.

Combining masked endocytic and COPI signals allows for regulated PM-to-ER transport

Thus far, we used two different strategies for masking of membrane traffic signals (creating a signal within SBP for endocytosis or appending a signal to SBP for COPI traffic). By combining the two strategies, one should be able to generate constructs in which the endocytic and COPI signals are masked simultaneously by SA. In light of the indication that the endocytosed $CD4_{1–429}$-SBP_{EL} construct can reach the Golgi (Figure 7D), we reasoned that a $CD4_{1–429}$-SBP_{EL}-K(X)KXX construct might travel all the way from the PM to the ER upon unmasking. To test this idea, we cotransfected HeLa cells with SA and $CD4_{1–429}$-SBP_{EL}-KRKAE and monitored anti-CD4 antibody uptake (Figure 8A). Significantly, upon incubation in the presence of biotin, the antibody became ER localized, as revealed by colocalization with the ER marker SRβ. ER redistribution

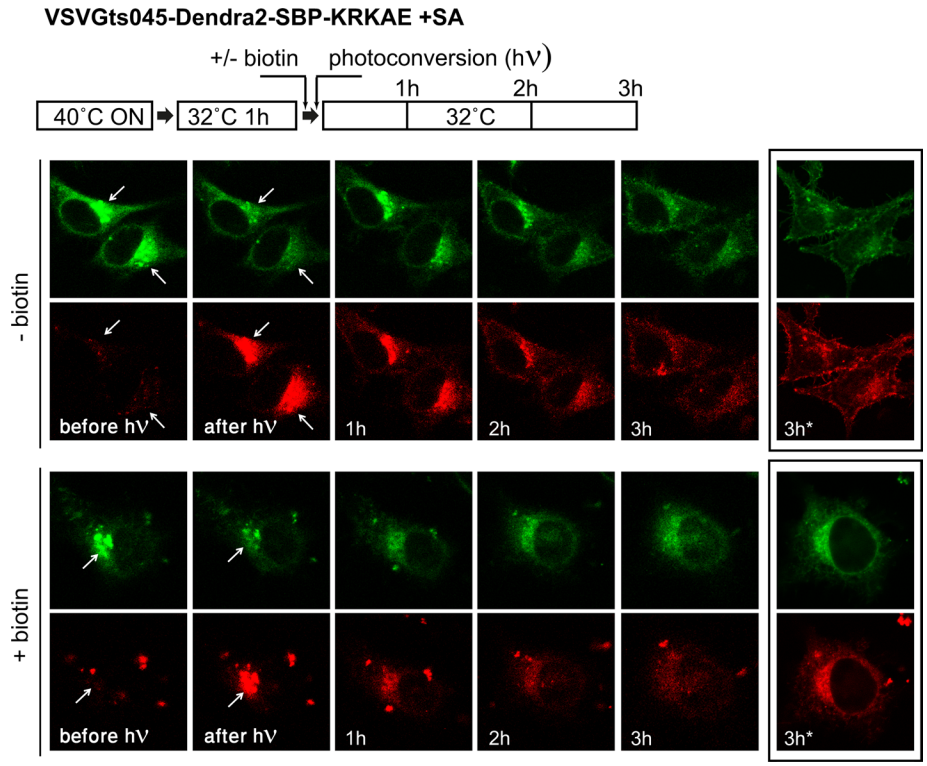

FIGURE 5: Golgi-to-ER retrieval of VSVGts045 followed with a photoconvertible fluorescent protein. Cells were cotransfected with VSVGts045-dendra2-SBP-KRKAE and SA. After overnight incubation at 40°C, the temperature was shifted to 32°C for 1 h to allow the VSVGts045 construct to reach the Golgi. The dendra2 protein was then photoconverted at the Golgi area, and the cells were followed by live imaging at 32°C. Biotin was added immediately before photoconversion (bottom lane). The images marked 3 h* were taken after refocusing for better clarity.

became evident at 2 h after the addition of biotin and was completed at 4 h, whereas in the absence of biotin, the antibody remained PM associated. We observed PM-to-ER transport with similar kinetics by live-cell imaging (Figure 8B). A complete redistribution of anti-CD4 antibody to the ER at 4 h after biotin addition was observed in virtually all cells examined. Both the endocytic and the COPI signals were required for PM-to-ER transport, as constructs lacking either signal failed to mediate anti-CD4 antibody transport to the ER at 4 h (Figure 8C). The observation that the construct with COPI signal only ($CD4_{1–429}$–SBP-KRKAE) remained PM associated upon biotin addition indicates that the COPI system is incapable of retrieving dilysine-tagged proteins from the PM.

Following endocytosis, a likely pathway for PM-to-ER transport involves retrograde transport from endosomes to the Golgi and from the Golgi to the ER. Indeed, when following the pathway of transport at 1 h, we observed some $CD4_{1–429}$-SBP_{EL}-KRKAE at the Golgi region (Figure 9A); however, colocalization of the construct with Golgi and TGN markers was rather low and was weaker than that of the same construct without the COPI signal (Figure 7D). At this point, much of $CD4_{1–429}$-SBP_{EL}-KRKAE colocalized with the early endosome marker EEA1 (Figure 9A). To investigate further the role of the Golgi in transport of $CD4_{1–429}$-SBP_{EL}-KRKAE from the PM to the ER, we tested the effect of two agents that disrupt the Golgi apparatus, brefeldin A (BFA) and golgicide A (GCA). These agents inhibit the recruitment of the COPI system to the Golgi through inhibition of Golgi-associated Arf1 guanine nucleotide exchange factors (Donaldson *et al.*, 1992; Helms and Rothman, 1992; Niu *et al.*, 2005; Saenz *et al.*, 2009) and induce a merge between the Golgi apparatus and the ER (Lippincott-Schwartz *et al.*, 1991). For BFA, we used a low concentration (0.2 μg/ml) that was reported as sufficient for disrupting the Golgi apparatus during prolonged incubations without interference with the endosomal system (Bershadsky and Futerman, 1994). Both GCA and BFA caused the redistribution of the medial/*trans*-Golgi enzyme GalT to the ER (Figure 9B). We treated cells expressing $CD4_{1–429}$-SBP_{EL}-KRKAE masked with SA simultaneously with biotin and the drugs during a 4-h incubation. In the presence of either drug, the construct showed a punctate pattern (Figure 9C), with significant colocalization with the endosomal marker EEA1 (Supplemental Figure S2), and transport to the ER was prevented. These findings indicate that PM-to-ER transport of our reporter depends on Golgi function and/or other Arf1-dependent processes operating at the Golgi.

Retrograde transport from endosomes to the TGN frequently involves retromer (Johannes and Popoff, 2008). However, knocking down the VPS26 subunit of retromer had no effect on biotin-induced ER delivery of $CD4_{1–429}$-SBP_{EL}-KRKAE (Supplemental Figure S3).

Modes of signal masking

Trafficking signals incorporated into the SBP sequence should be directly masked upon SA binding, whereas in the case of signals appended at the SBP carboxy terminus, we expected masking due to steric interference by which the tetrameric SA excludes receptor/coat binding to the proximal trafficking signal; however, other indirect mechanisms could not be excluded. If masking is due to steric interference, it should be abrogated by increasing the distance between SBP and the appended signal. This was tested by inserting flexible linkers between SBP and the signals (Figure 10). As expected for steric interference, insertion of a 10-aa linker abolished the masking of the NLS signal by SA. However, linker insertion did not prevent masking of the peroxisomal and COPI signals. This was the case even when the length of the linker between SBP and the dilysine COPI signal was increased to 20 aa (Figure 10, lnkx2). Thus the observed abrogation of the peroxisomal and COPI-mediated transport may be due to mechanisms other than direct interference with receptor binding.

DISCUSSION

We demonstrated the feasibility of a CUTE approach for control of the timing of diverse intracellular transport processes, including both protein import from cytosol into the nucleus and peroxisomes and vesicular trafficking (COPI-mediated retrograde transport and endocytosis). Advantages of the CUTE system in comparison to other approaches for regulating protein trafficking include the relatively short tag that is attached to the reporter (SBP), the use of a single agent (soluble streptavidin) to mask multiple transport signals, and the fact that membrane hooks are not required. The reversible masking approach is particularly useful in the case of retrograde transport in the secretory system because in hook–reporter systems (Boncompain *et al.*, 2012), the presence of

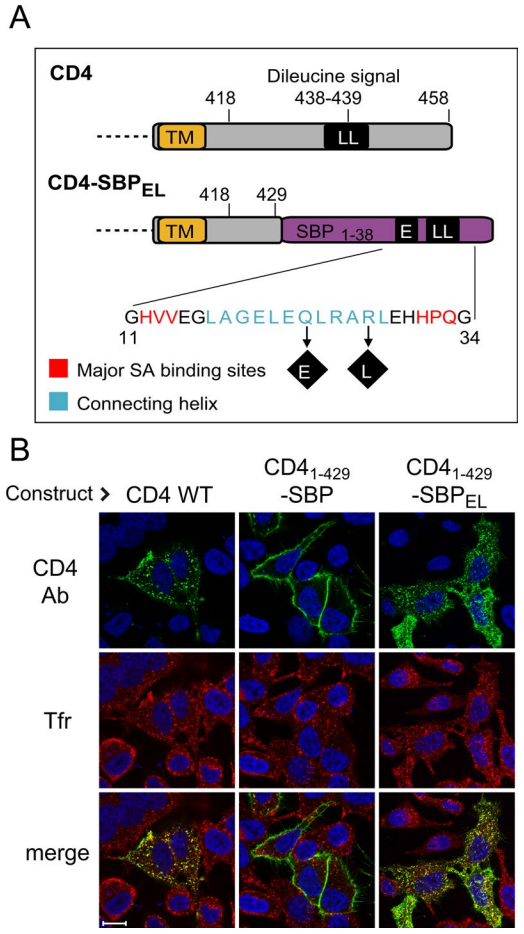

FIGURE 6: Generation of endocytic signal within SBP. (A) Scheme of the construct used for regulated endocytosis. Most of the cytosolic domain of CD4 (top) was replaced with a modified SBP (SBP_{EL}) containing two amino acid replacements that generate an acidic-dileucine endocytic signal (ELRALL). TM, transmembrane domain. (B) The engineered signal mediates endocytic traffic. Cells were transfected with the indicated constructs. At 24 h later, cells were incubated in the cold with Alexa 488–conjugated anti-CD4 antibodies, followed by 20 min of incubation at 37°C in the presence of 20 ng/ml Texas Red–conjugated transferrin; cells expressing wild-type CD4 also received 100 ng/ml PMA (Pitcher *et al.*, 1999). Cells were fixed, and nuclei were stained with Hoechst.

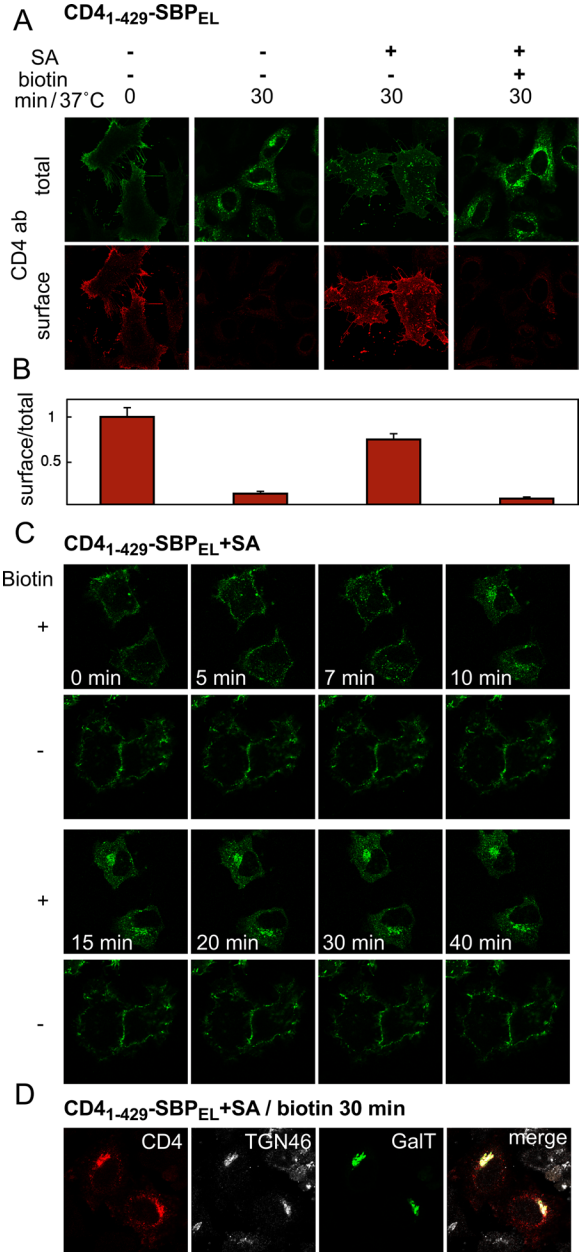

FIGURE 7: Reversible masking of an endocytic signal embedded in SBP. (A) Quantitative assessment of $CD4_{1–429}$-SBP_{EL} internalization. Cells were transfected with $CD4_{1–429}$-SBP_{EL} with or without SA, incubated with Alexa 488–conjugated anti-CD4 antibody with or without biotin, fixed (but not permeabilized), and stained with cy3-conjugated secondary antibody to reveal the presence of anti-CD4 antibodies at the surface. (B) Quantification of endocytic transport. Cells were treated as in A and analyzed for total fluorescence (Alexa 488-anti CD4) and surface fluorescence (CY3-conjugated secondary antibody) using an In Cell analyzer (see *Materials and Methods*); the normalized ratios between surface and total fluorescence are presented, with each bar representing cells treated as indicated on the image above it in A. (C) Live imaging of biotin-induced endocytosis. Cells were cotransfected with $CD4_{1–429}$-SBP_{EL} and SA (1:1). Uptake of Alexa 488–conjugated anti-CD4 antibodies in the presence or absence of biotin was followed by live imaging. (D) $CD4_{1–429}$-SBP_{EL} reaches the Golgi area. Cells were cotransfected with SA, $CD4_{1–429}$-SBP_{EL}, and GalT-CFP (1:1:0.25). After 30 min of incubation in the presence of biotin, endocytosed monoclonal anti-CD4 antibodies were detected with secondary antibody; TGN46 was detected with specific polyclonal antibodies.

exposed retrograde signal on the reporter may prevent the arrival of the coexpressed hook to the sequestering organelle. This is particularly true in the case of the two-way ER/Golgi transport, for which reporters bearing strong COPI signals show a largely ER distribution at steady state (Zerangue *et al.*, 2001). By masking dilysine COPI signals, we were able to allow post-ER transport of the retrograde traffic reporter. However, to study retrograde COPI traffic, one has to prevent transport of the reporter beyond the range of the COPI system, which is unable to retrieve proteins that have reached the plasma membrane (Figure 8C). This was achieved by limiting anterograde transport of VSVGts045-based reporters using a short incubation at the permissive temperature before biotin addition. Ideally, one would use a Golgi- resident protein with appended dilysine signal as reporter for COPI traffic, but so far our attempts to generate such a reporter using some of the relatively scarce Golgi/TGN type I resident proteins have not met with success.

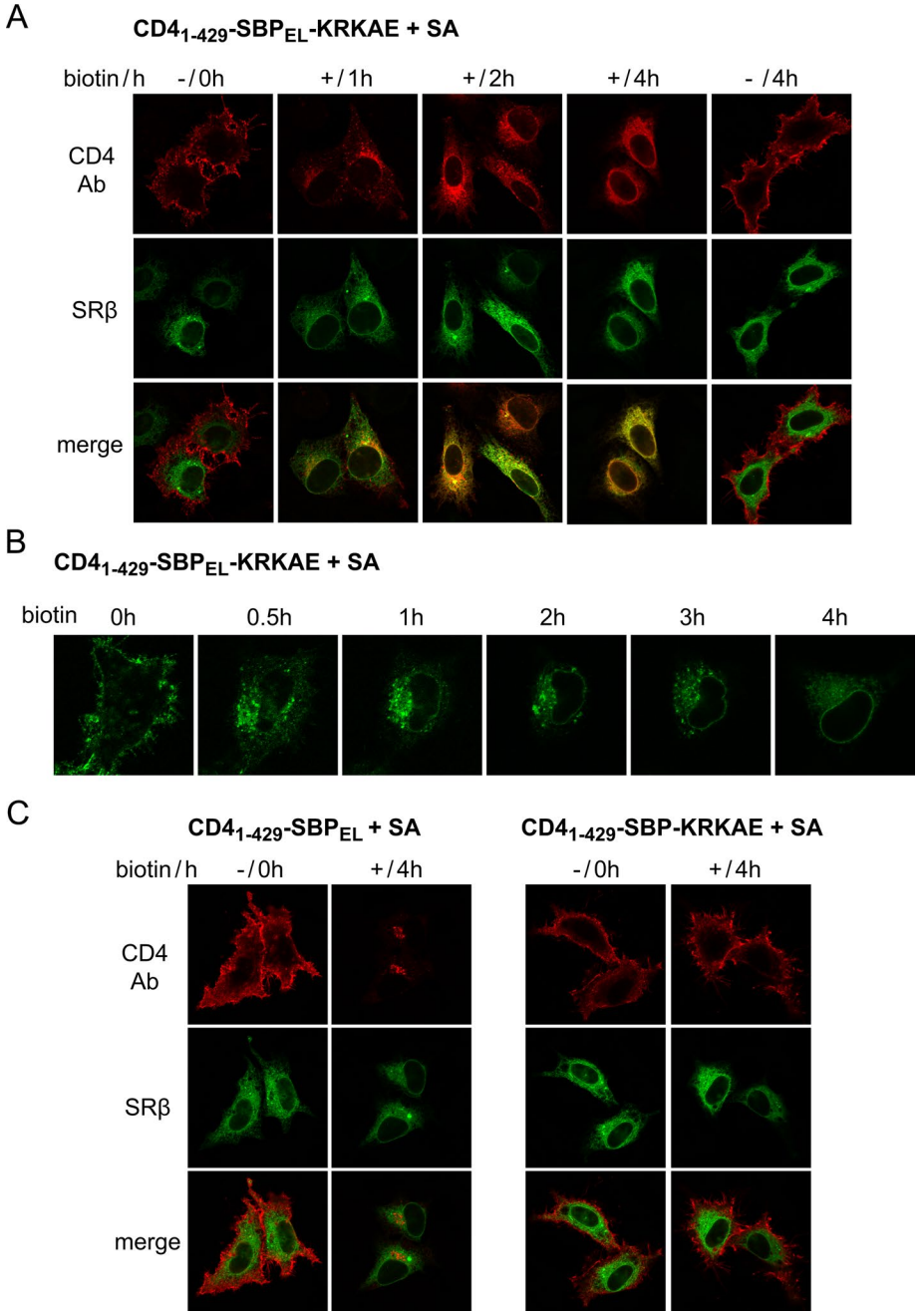

FIGURE 8: Controlled transport of plasma membrane reporter to the ER. Cells were cotransfected with CD4$_{1-429}$-SBP–based constructs and SA (1:1). After 24 h, cells were incubated with anti-CD4 antibodies in the cold, washed, and incubated at 37°C for the indicated times with or without biotin. (A, C) Cells cotransfected with CFP-SRβ were fixed and stained with CY3-conjugated secondary antibody. (B) Uptake of Alexa 488–conjugated anti-CD4 antibody was followed by live imaging.

The application of the SBP-SA interaction for studies of cellular processes relies on the high affinity of this interaction (K_d = 2 nM; Wilson *et al.*, 2001), which is in large part due to simultaneous binding of two amino acid triplets on SBP to two biotin-binding sites in the tetrameric SA (Barrette-Ng *et al.*, 2013). Our attempts to mask trafficking signals relied on either appending the signal to the carboxy side of SBP or generating a signal by mutating the 16-aa sequence that links the two major SA-binding sites. The latter approach, which we successfully used for generating an endocytic signal, should be optimal whenever the signal of interest can be produced by amino acid substitutions in SBP that do not result in significant reduction in its affinity for SA. This approach, however, is not applicable to signals that must be present at the carboxy extremity of the protein (e.g., the dilysine and SKL motifs used in this study). In the latter cases, as well as with NLS signals, we used the other approach by which the signals were appended to SBP. Initially, we attempted to append the signals immediately after the HPQ(G) sequence that constitutes the carboxy SA-interaction motif; however, unexpectedly, masking of dilysine signals with this construct was less efficient than with full-length SBP, which has additional 4 aa at the carboxy side, even though these amino acids are not critical for SA interaction. To further explore the masking mechanism, we tested the effect of the introduction of linkers between SBP and trafficking signals (Figure 10). In the case of the polybasic NLS, signal masking was abolished by linker introduction, indicating that masking requires proximity of the NLS to the bound SA, which presumably leads to steric interference with the binding of nuclear import receptors. By contrast, there was no effect of linkers on the masking of COPI K(X)KXX and peroxisomal SKL signals, indicating that in these two cases, masking is due to mechanisms other than steric interference with receptor binding. A possible explanation for the masking of the COPI signal observed even in a construct containing a long linker (20 aa) may involve a previously reported negative effect of increased membrane distance on the efficiency of dilysine signals (Shikano and Li, 2003). Perhaps binding of the structured tetrameric SA to SBP-K(X)KXX prevents efficient approach of the dilysine signal to the membrane to allow for sorting into COPI vesicles. Whatever the mechanism, in practice, masking of both COPI dilysine and peroxisomal SKL signals by our approach is efficient and reversible, making our approach useful for transport synchronization.

By the simultaneous masking of COPI and endocytic signals, we could allow a reporter to accumulate at the plasma membrane and subsequently trigger its highly efficient transport all the way back to the ER (Figure 8). In principle, this synthetic PM-to-ER transport could be mediated by a combination of known endocytic, endosome-to-TGN and COPI-mediated pathways. Consistent with this idea are the observations that the construct containing the synthetic endocytic signal that we generated in SBP partially localized at the Golgi and that ER transport of the construct with both endocytic and COPI signals was prevented by agents that disrupt the Golgi (Figure 9). The rather long duration of completion of PM-to-ER transport (~4 h) might result from a rate-limiting step along the transport pathway; this could be retrograde

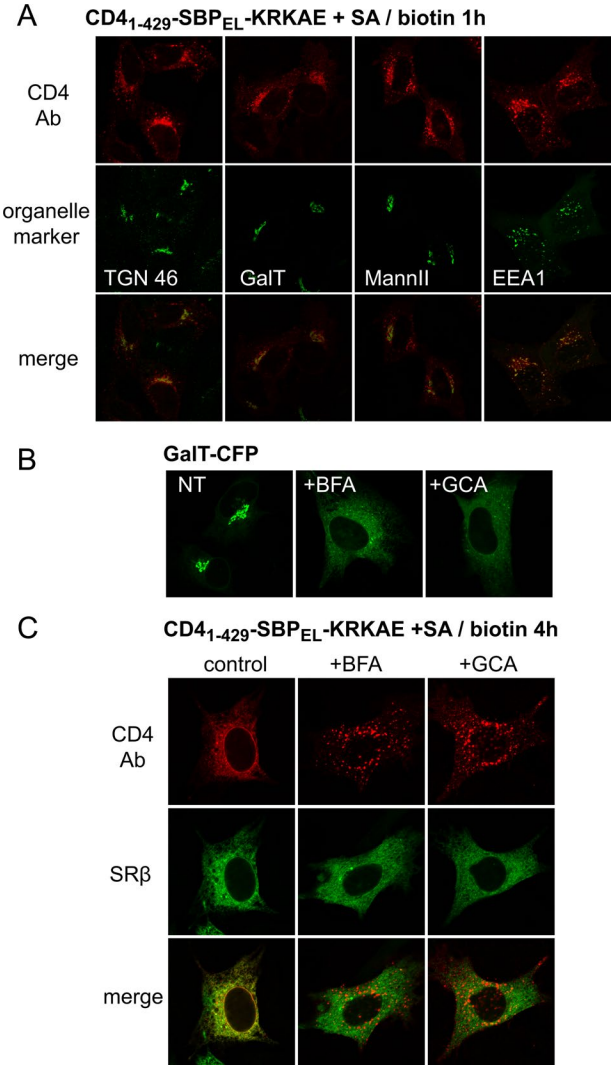

FIGURE 9: Role of the Golgi apparatus in PM-to-ER transport of CD4$_{1–429}$-SBP$_{EL}$-KRKAE. (A) CD4$_{1–429}$-SBP$_{EL}$-KRKAE partially colocalizes with Golgi and endosomal markers after 1 h of biotin treatment. Organelle markers GalT-CFP, GFP-ManII, and GFP-EEA1 were introduced by plasmid transfection, and TGN was detected using anti-TGN46 antibodies. (B) BFA (0.2 µg/ml) and GCA (5 µg/ml) cause the dispersal of the Golgi marker GalT into the ER after 4 h of incubation. NT, nontreated. (C) BFA and GCA block biotin-induced transfer of CD4$_{1–429}$-SBP$_{EL}$-KRKAE to the ER. Cells were incubated with biotin for 4 h in the presence or absence of BFA or GCA and were processed as in Figure 8A.

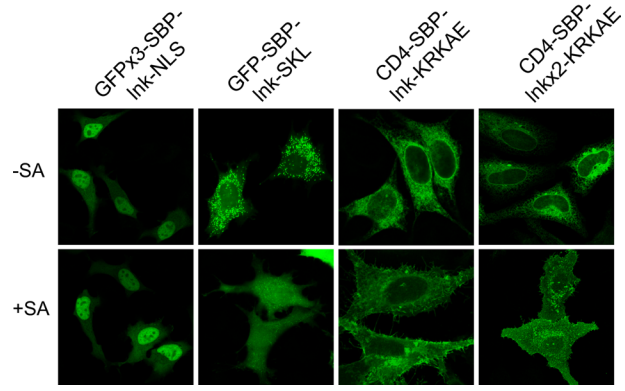

FIGURE 10: Effect of the insertion of linkers between SBP and the targeting signals. Cells were transfected with the indicated constructs with or without streptavidin and incubated for 24 h at 37°C; for CD4 constructs, cells were permeabilized and stained with anti-CD4 antibodies. lnk, GGGGSGGGGS; lnkx2, GGGGSGGGGSGGG-GSGGGGS.

endosome-to-Golgi transport, as suggested by the significant endosomal presence of CD4-SBP/LE-KRKAE during intermediate stages of transport.

Transport routes from the PM to the ER are known for several bacterial toxins and viral proteins (Sandvig *et al.*, 2013). These pathways are quite varied and may or may not involve passage through the TGN/Golgi cisternae. Recently evidence for cycling of plasma membrane proteins through the ER was provided using the SNAP-tag approach for ER trapping (Geiger *et al.*, 2013). Future studies should reveal whether the synthetic pathway that we generated and the natural pathways share some common mechanisms.

Delivery of extracellular factors to the ER may have implementations in both basic and translational research—for example, for antigen presentation (Wang *et al.*, 2004). Our CUTE system, or modifications thereof, may provide an alternative way for controlled and specific delivery of membrane-impermeable substances such as peptides and antibodies to the ER using modified membrane receptors.

MATERIALS AND METHODS

Generation of DNA constructs for mammalian cell expression

A GFPx3 construct was prepared by inserting two GFP cDNAs into the pEGFPC1 plasmid (Clontech, Mountain View, CA) using *Xho*I/*Hin*dIII and *Hin*dIII/*Eco*RI. The sequence encoding SBP (Wilson *et al.*, 2001) followed by the SV40 large T antigen NLS (KKKRKV) was then inserted into the *Eco*RI/*Bam*HI sites. GFP-SBP-SKL was similarly prepared using the original pEGFPC1 plasmid. VSVGts045-GFP and VSVGts045-Dendra2 were prepared by inserting the PCR-amplified VSVGts045 sequence between the *Nhe*I and *Age*I sites of pEGFP-C2 or pDendra2. SBP with appended K(X)KXX signals was then introduced between the *Xho*I and *Bam*HI or *Eco*RI and *Bam*HI sites for pEGFP and pDendra2, respectively. To generate CD4-GFP-SBP-K(X)KXX constructs, the GFP-SBP-K(X)KXX sequence was PCR amplified from the corresponding VSVGts045 constructs and cloned between the *Not*I and *Xba*I sites of a CD4 construct in pCDNA3 (Yuan *et al.*, 2003). To introduce flexible linkers between SBP and the dilysine signal, DNAs encoding SBP-lnk-KRKAE were synthesized by IDT and cloned into CD4-GFP-SBP-KRKAE cut with *Xho*I and *Xba*I. To generate a CD4-based construct for controllable endocytosis, the carboxy tail of CD4 (including the endocytic signal) was truncated down to amino acid 429; SBP or its derivatives with Q23E/R27L replacements and with a carboxy-terminal KRKAE sequence were cloned between *Not*I and *Xba*I. To generate the soluble streptavidin construct, the core streptavidin was amplified by PCR using oligos GATCGGATCCT-TACTGCTGGACGGCATCCAG (forward) and GAATTGCTAGCGC-CACCATGGACCCTAGCAAAGACTC (reverse) and a RUSH plasmid as template (Boncompain *et al.*, 2012). The PCR product was inserted into a pIRESpuro3 vector (from Clontech) using *Nhe*I and *Bam*HI restriction enzymes. Plasmids encoding organelle markers were provided by Koret Hirschberg (Faculty of Medicine, Tel Aviv University).

Transfection and immunofluorescence microscopy

HeLa cells grown in DMEM/10% fetal calf serum/5 mM pyruvate on 13-mm glass coverslips inside 24-well plates were transfected with

plasmids (0.5 µg total) using 1.8 µl of FuGENE-HD (Promega, Madison, WI) or 1 µg of DNA and 2 µl of jetPEI (Polyplus, Strasbourg, France; for NLS plasmids only) according to manufacturer's instructions. When cotransfected, the ratio between SBP plasmids and streptavidin was titrated and optimized for each SBP construct and is indicated in the figure legends. Experiments were initiated 20–24 h after transfection. Where indicated, 400 µM biotin and 20 µg/ml cycloheximide were added. Cells were fixed with 4% paraformaldehyde. For immunostaining, cells were permeabilized by treatment with phosphate-buffered saline (PBS) containing 0.05% saponin and 0.2% bovine serum albumin and incubated with primary antibodies (mouse anti-GM130 [Bactlab Diagnostics, Caeserea, Israel; 1:400; rabbit anti-TGN46 [Abcam, Cambridge, UK], 1:100; mouse anti-CD4 [Santa Cruz Biotechnology, Dallas, TX], 1:250; mouse anti-streptavidin [Santa Cruz Biotechnology], 1:500), rabbit anti-VPS26 [Abcam], 1:100) followed by Cy3-, Cy5-, or Alexa 488–conjugated secondary antibodies. For selective plasma membrane staining, cells were treated similarly but in the absence of saponin. Coverslips were mounted on glass slides using Mowiol as glue, and cells were visualized under an LSM710 confocal inverted fluorescence microscope (Zeiss, Oberkochen, Germany) with a Plan-Apochromat 63×/1.4 differential interference contrast oil objective. Scale bars in all images are 10 µm. The experiments were repeated at least three times with similar results. The variation between individual cells under each experimental condition was determined by observing the phenotype in 100–150 cells in each of two independent experiments; with the exception of nuclear import (Figure 2B), the reported phenotype was observed in >94% of the cells.

Following CD4 internalization

At 24 h after transfection, cells were incubated on ice for 1 h with anti-CD4 antibodies (1:100) and then washed with cold culture medium. Biotin- and Texas Red–conjugated transferrin (Rockland, Limerick, PA) were added where indicated, and incubation proceeded at 37°C. For direct follow-up, we used Alexa Fluor 488–conjugated mouse monoclonal anti-CD4 antibody (SC19641-AF 488; Santa Cruz Biotechnology). Alternatively, we used the nonconjugated form of the same antibody (SC19641); after incubation at 37°C cells were fixed, permeabilized, and stained with Cy3-conjugated donkey anti-mouse antibodies.

Quantification of nuclear import and CD4 internalization

Nuclear localization of GFPX3-SBP-NLS was determined as a ratio between nuclear and cytosolic fluorescence. This was measured as the ratio of the total fluorescence within a circle with an area of ~9 µm^2 drawn inside the nucleus (avoiding the nucleolus) and that within the same circle drawn in a cytosolic area close to the nucleus. Background values taken in the same way from cell surrounding were deducted.

For quantitative assessment of CD4 internalization, after incubation with the Alexa Fluor 488–conjugated anti-CD4 antibody, cells were washed and fixed, and the remaining surface CD4-bound antibody was stained with cy3-conjugated donkey anti-mouse antibody; nuclei were stained with Hoechst. Multiple images were taken using a GE In Cell 2000 analyzer (GE Healthcare, Pittsburgh, PA). The range of measurement was automatically defined as that encompassed by a line drawn around the nucleus at a distance of 3 µm, and average red and green fluorescence within this area was determined. After background deduction, the ratio between the combined average fluorescence in the red channel (external antibody) and green channel (total antibody) was determined, and values were normalized relatively to the zero time value. Between 2000 and 7000 cells were used under each condition, and values are presented as mean ± SD of three different wells.

Live-cell imaging

HeLa cells grown on 35-mm glass-bottom dishes (Greiner Bio-One, Frickenhausen, Germany) were transfected with of 2.5 µg of plasmid DNA and viewed under the LSM710 microscope. To follow CD4 internalization, cells were preincubated for 1 h on ice with Alexa 488–conjugated anti-CD4 antibody (SC19641 AF488,1:100; Santa Cruz Biotechnology); cells displaying relatively weak expression were selected for imaging. For Dendra2 experiments, the fluorescent protein was photoconverted by irradiation with a 405-nm laser line for 1.27 µs by 250 repeats with 5% laser intensity (maximal laser intensity in the LSM710 microscope, 25 mW). The redistribution of Dendra2 was tracked at excitation 490 nm/emission 507 nm (unactivated) and excitation 553 nm/emission 573 nm (activated).

ACKNOWLEDGMENTS

We thank Blanche Schwappach and Daniel Kaganovich for plasmids and Fabian Glaser and Michael Shmoish for help in bioinformatics and statistical analysis. This work was supported by a grant to D.C. from the Israel Science Foundation (2020030) and an award from the Skillman Foundation.

REFERENCES

Al-Bassam S, Xu M, Wandless TJ, Arnold DB (2012). Differential trafficking of transport vesicles contributes to the localization of dendritic proteins. Cell Rep 2, 89–100.

Barrette-Ng IH, Wu SC, Tjia WM, Wong SL, Ng KK (2013). The structure of the SBP-Tag-streptavidin complex reveals a novel helical scaffold bridging binding pockets on separate subunits. Acta Crystallogr D Biol Crystallogr 69, 879–887.

Bergmann JE (1989). Using temperature-sensitive mutants of VSV to study membrane protein biogenesis. Methods Cell Biol 32, 85–110.

Bergmann JE, Tokuyasu KT, Singer SJ (1981). Passage of an integral membrane protein, the vesicular stomatitis virus glycoprotein, through the Golgi apparatus en route to the plasma membrane. Proc Natl Acad Sci USA 78, 1746–1750.

Bershadsky AD, Futerman AH (1994). Disruption of the Golgi apparatus by brefeldin A blocks cell polarization and inhibits directed cell migration. Proc Natl Acad Sci USA 91, 5686–5689.

Beyer HM, Juillot S, Herbst K, Samodelov SL, Muller K, Schamel WW, Romer W, Schafer E, Nagy F, Strahle U, *et al*. (2015). Red light-regulated reversible nuclear localization of proteins in mammalian cells and zebrafish. ACS Synth Biol 4, 951–958.

Boncompain G, Divoux S, Gareil N, de Forges H, Lescure A, Latreche L, Mercanti V, Jollivet F, Raposo G, Perez F (2012). Synchronization of secretory protein traffic in populations of cells. Nat Methods 9, 493–498.

Bonifacino JS, Traub LM (2003). Signals for sorting of transmembrane proteins to endosomes and lysosomes. Annu Rev Biochem 72, 395–447.

Chen D, Gibson ES, Kennedy MJ (2013). A light-triggered protein secretion system. J Cell Biol 201, 631–640.

Donaldson JG, Finazzi D, Klausner RD (1992). Brefeldin A inhibits Golgi membrane-catalysed exchange of guanine nucleotide onto ARF protein. Nature 360, 350–352.

Geda P, Patury S, Ma J, Bharucha N, Dobry CJ, Lawson SK, Gestwicki JE, Kumar A (2008). A small molecule-directed approach to control protein localization and function. Yeast 25, 577–594.

Geiger R, Luisoni S, Johnsson K, Greber UF, Helenius A (2013). Investigating endocytic pathways to the endoplasmic reticulum and to the cytosol using SNAP-trap. Traffic 14, 36–46.

Griffiths G, Fuller SD, Back R, Hollinshead M, Pfeiffer S, Simons K (1989). The dynamic nature of the Golgi complex. J Cell Biol 108, 277–297.

Helms JB, Rothman JE (1992). Inhibition by brefeldin A of a Golgi membrane enzyme that catalyses exchange of guanine nucleotide bound to ARF. Nature 360, 352–354.

Jackson LP, Lewis M, Kent HM, Edeling MA, Evans PR, Duden R, Owen DJ (2012). Molecular basis for recognition of dilysine trafficking motifs by COPI. Dev Cell 23, 1255–1262.

Johannes L, Popoff V (2008). Tracing the retrograde route in protein trafficking. Cell 135, 1175–1187.

Klumperman J, Schweizer A, Clausen H, Tang BL, Hong W, Oorschot V, Hauri HP (1998). The recycling pathway of protein ERGIC-53 and dynamics of the ER-Golgi intermediate compartment. J Cell Sci 111, 3411–3425.
Letourneur F, Gaynor EC, Hennecke S, Demolliere C, Duden R, Emr SD, Riezman H, Cosson P (1994). Coatomer is essential for retrieval of dilysine-tagged proteins to the endoplasmic reticulum. Cell 79, 1199–1207.
Lippincott-Schwartz J, Yuan L, Tipper C, Amherdt M, Orci L, Klausner RD (1991). Brefeldin A's effects on endosomes, lysosomes, and the TGN suggest a general mechanism for regulating organelle structure and membrane traffic. Cell 67, 601–616.
Lodish HF, Kong N (1983). Reversible block in intracellular transport and budding of mutant vesicular stomatitis virus glycoproteins. Virology 125, 335–348.
Lotti LV, Torrisi MR, Pascale MC, Bonatti S (1992). Immunocytochemical analysis of the transfer of vesicular stomatitis virus G glycoprotein from the intermediate compartment to the Golgi complex. J Cell Biol 118, 43–50.
Ma W, Goldberg J (2013). Rules for the recognition of dilysine retrieval motifs by coatomer. EMBO J 32, 926–937.
Matlin KS, Simons K (1983). Reduced temperature prevents transfer of a membrane glycoprotein to the cell surface but does not prevent terminal glycosylation. Cell 34, 233–243.
Niu TK, Pfeifer AC, Lippincott-Schwartz J, Jackson CL (2005). Dynamics of GBF1, a brefeldin A-sensitive Arf1 exchange factor at the Golgi. Mol Biol Cell 16, 1213–1222.
Pandey KN (2010). Small peptide recognition sequence for intracellular sorting. Curr Opin Biotechnol 21, 611–620.
Pettersen EF, Goddard TD, Huang CC, Couch GS, Greenblatt DM, Meng EC, Ferrin TE (2004). UCSF Chimera—a visualization system for exploratory research and analysis. J Comput Chem 25, 1605–1612.
Pitcher C, Honing S, Fingerhut A, Bowers K, Marsh M (1999). Cluster of differentiation antigen 4 (CD4) endocytosis and adaptor complex binding require activation of the CD4 endocytosis signal by serine phosphorylation. Mol Biol Cell 10, 677–691.
Presley JF, Cole NB, Schroer TA, Hirschberg K, Zaal KJ, Lippincott-Schwartz J (1997). ER-to-Golgi transport visualized in living cells. Nature 389, 81–85.
Rakhit R, Navarro R, Wandless TJ (2014). Chemical biology strategies for posttranslational control of protein function. Chem Biol 21, 1238–1252.
Rivera VM, Wang X, Wardwell S, Courage NL, Volchuk A, Keenan T, Holt DA, Gilman M, Orci L, Cerasoli F, *et al*. (2000). Regulation of protein secretion through controlled aggregation in the endoplasmic reticulum. Science 287, 826–830.
Saenz JB, Sun WJ, Chang JW, Li J, Bursulaya B, Gray NS, Haslam DB (2009). Golgicide A reveals essential roles for GBF1 in Golgi assembly and function. Nat Chem Biol 5, 157–165.
Sakakida Y, Miyamoto Y, Nagoshi E, Akashi M, Nakamura TJ, Mamine T, Kasahara M, Minami Y, Yoneda Y, Takumi T (2005). Importin alpha/beta mediates nuclear transport of a mammalian circadian clock component, mCRY2, together with mPER2, through a bipartite nuclear localization signal. J Biol Chem 280, 13272–13278.
Sandvig K, Skotland T, van Deurs B, Klokk TI (2013). Retrograde transport of protein toxins through the Golgi apparatus. Histochem Cell Biol 140, 317–326.
Saraste J, Kuismanen E (1984). Pre- and post-Golgi vacuoles operate in the transport of Semliki Forest virus membrane glycoproteins to the cell surface. Cell 38, 535–549.
Saraste J, Palade GE, Farquhar MG (1986). Temperature-sensitive steps in the transport of secretory proteins through the Golgi complex in exocrine pancreatic cells. Proc Natl Acad Sci USA 83, 6425–6429.
Shikano S, Li M (2003). Membrane receptor trafficking: evidence of proximal and distal zones conferred by two independent endoplasmic reticulum localization signals. Proc Natl Acad Sci USA 100, 5783–5788.
Smith JJ, Aitchison JD (2013). Peroxisomes take shape. Nat Rev Mol Cell Biol 14, 803–817.
Walton PA, Gould SJ, Feramisco JR, Subramani S (1992). Transport of microinjected proteins into peroxisomes of mammalian cells: inability of Zellweger cell lines to import proteins with the SKL tripeptide peroxisomal targeting signal. Mol Cell Biol 12, 531–541.
Wang L, Wu YZ, Chen A, Zhang JB, Yang Z, Niu W, Geng M, Ni B, Zhou W, Zou LY, *et al*. (2004). MHC class I-associated presentation of exogenous peptides is not only enhanced but also prolonged by linking with a C-terminal Lys-Asp-Glu-Leu endoplasmic reticulum retrieval signal. Eur J Immunol 34, 3582–3594.
Wilson DS, Keefe AD, Szostak JW (2001). The use of mRNA display to select high-affinity protein-binding peptides. Proc Natl Acad Sci USA 98, 3750–3755.
Yuan H, Michelsen K, Schwappach B (2003). 14-3-3 dimers probe the assembly status of multimeric membrane proteins. Curr Biol 13, 638–646.
Zerangue N, Malan MJ, Fried SR, Dazin PF, Jan YN, Jan LY, Schwappach B (2001). Analysis of endoplasmic reticulum trafficking signals by combinatorial screening in mammalian cells. Proc Natl Acad Sci USA 98, 2431–2436.